Influence of Incorporation of ZnO Nanoparticles and Biaxial Orientation on Mechanical and Oxygen Barrier Properties of Polypropylene Films for Food Packaging Applications

N. Lepot,[1,2] M. K. Van Bael,[1,3] H. Van den Rul,[1] J. D'Haen,[1,4] R. Peeters,[2] D. Franco,[2] J. Mullens[1]

[1]*Hasselt University, Institute for Materials Research, Inorganic and Physical Chemistry, Diepenbeek, Belgium*
[2]*Xios Hogeschool Limburg, Verpakkingscentrum, Universitaire Campus Diepenbeek, Diepenbeek, Belgium*
[3]*IMEC vzw, Division IMOMEC, Diepenbeek, Belgium*
[4]*Hasselt University, Institute for Materials Research, Diepenbeek, Belgium*

Received 9 July 2009; accepted 6 March 2010
DOI 10.1002/app.33277
Published online 1 December 2010 in Wiley Online Library (wileyonlinelibrary.com).

ABSTRACT: In this work, the effect of zinc oxide (ZnO) concentration and shape on processing and properties of new biaxially oriented polypropylene (BOPP)-ZnO nanocomposites was studied. The use of spherical nanoparticles and nanorods was expected to differently influence the properties of the final material. Films of isotactic polypropylene prepared with different ZnO incorporation were biaxially oriented under conditions of temperature and strain rate that were similar to those encountered in a commercial film process. Scanning electron microscopy analysis was performed to visualize the dispersion degree of the ZnO nanoparticles in the polymer matrix and to observe the surface and the orientation of the elongated nanoparticles. Furthermore, the prepared ZnO-BOPP nanocomposites were evaluated for both mechanical and oxygen barrier property enhancement. A good combination of mechanical and oxygen barrier properties was obtained for the ZnO-BOPP films. This result makes the ZnO-BOPP nanocomposite a proper material for applications such as food packaging. © 2010 Wiley Periodicals, Inc. J Appl Polym Sci 120: 1616–1623, 2011

Key words: ZnO-BOPP nanocomposites; tensile strength; gas transport

INTRODUCTION

The very large commercial importance of polymers has been driving an intense investigation in polymers combined with particles, fibers, etc.[1–4] The interest in nanocomposites is due to their remarkable properties compared with conventional composites. Polymer nanocomposites are a class of materials that are particle-filled, with at least one dimension in the nanometer range. These nanoparticles are dispersed in the polymer matrix at a relatively low wt % (often less than 10% by weight). In general, nanoparticles can significantly improve mechanical properties, thermal stability, gas barrier properties, and/or flame retardancy of the polymer matrix.[3,5–8]

Among the polymer nanocomposites, those based on isotactic polypropylene (iPP) have attracted considerable interest because iPP is one of the most important commercial polymers because of its low price and attractive combination of good processability, mechanical properties, and chemical resistance.[9,10] Furthermore, PP films are used in packaging applications because of their good barrier properties, strength, and transparency.[3,11,12] The biaxial stretching of the material either in one single step or sequentially is a fundamental step in the production of polypropylene films for packaging applications. Orientation of polypropylene involves a morphological transformation of spherulites into a network of microfibrils and reduces the gas permeability of polypropylene.[13–15]

Compounding iPP with inorganic particles is an effective method to improve the properties of iPP. In the past decade, one of the most intensively studied composite systems was that based on organic polymers and inorganic clay minerals consisting of silicate layers.[16,17] Because of the difference in polarity between the polypropylene (nonpolar) and the filler (polar), different methods can be followed to improve the miscibility between the clay and the polymer, i.e., the fillers can be modified by organic compounds, and functional compounds can be used as compatibilizer.[18,19] Besides nanoclay, zinc oxide (ZnO),[20] silica,[21] and calcium carbonate[22] nanoparticles are used in iPP. Melt compounding,[23,24]

Correspondence to: J. Mullens (jules.mullens@uhasselt.be).
Contract grant sponsor: Fund for Scientific Research of Flanders (FWO Vlaanderen) (to M. K. V. B.).

solution blending, and *in situ* polymerization[6] are well-established methods for preparing polypropylene nanocomposites. Among these various strategies, melt mixing is probably the most versatile technique used for the preparation of iPP nanocomposites.

In this article, the preparation of new biaxially oriented polypropylene (BOPP)-ZnO nanocomposites by melt compounding is described. From recent reports it is obvious that the dispersion of an inorganic filler in a thermoplastic material is not easy through a melt mixing process. The problem is even more severe when using nanoparticles because of their strong tendency to agglomerate. A good dispersion can be achieved by appropriate processing conditions and the use of either coupling agents or compatibilizers.[6,25–27] The effort in this work was focused on obtaining well-dispersed nanoparticles without the use of compatibilizers. The effect of the ZnO concentration and shape on the processing, the morphology, and the mechanical and barrier properties of the ZnO-BOPP nanocomposites is studied. The use of either spherical or elongated nanoparticles is expected to differently influence the properties of the final material.

Recently, some authors reported on the use of ZnO nanoparticles in polypropylene. Tang et al.[20] reported on the use of ZnO as good nucleating agent and studied how ZnO nanoparticles coated with organic nucleating agents affect the morphology and crystallization of iPP. Zhao and Li[28] did research on the use of ZnO as ultraviolet absorber in polypropylene. To obtain a uniform dispersion in the polymer matrix, surface treatment of the ZnO nanoparticles with a silane coupling agent was necessary. Huang et al.[26] added ZnO nanopowder through microinjection molding to investigate the mechanical properties of polypropylene. However, the use of dispersants was necessary to obtain a good dispersion of the nanoparticles in the polymer matrix.

To our knowledge, no results were reported on the effect of the dispersion of ZnO nanoparticles without compatibilizer or coupling agent in a polypropylene matrix and its effect on mechanical and barrier properties after biaxial stretching of iPP.

EXPERIMENTAL

Materials

Isotactic polypropylene with melt flow index of 3 g/10 min and density 905 kg/m^3 as the polymer matrix, the antioxidant Irganox 1010, and the acid scavenger calcium stearate were supplied by Borealis Polymers NV (Beringen, Belgium).

Spherical ZnO nanoparticles were purchased from Aldrich Chemicals (St. Louis, MO) with average primary particle size 50–70 nm and specific surface area 15–25 m^2/g as specified by the supplier. Nanorods of ZnO with diameters of 50–200 nm and lengths up to 5 μm were synthesized using the procedure earlier described.[29] The hydrothermal technique described in this study has proved to be a successful method for the preparation of crystalline one-dimensional (1D) ZnO nanopowder by using water as the only solvent at a temperature of 80°C and zinc acetate dihydrate as the zinc source.

Nanocomposite preparation

In this study 0, 2, 5, and 7.5 wt % ZnO nanoparticles were incorporated in the polymer matrix. Because nanoparticles (such as nanoclays, nanofibers, etc.) are small and their aspect ratios (largest dimension/smallest dimension) can be high, even at such low loadings (<10 wt %) certain polymer properties can be greatly improved without a detrimental impact on density, transparency, and processability associated with conventional reinforcements like talc or glass.[6,8]

ZnO-polypropylene nanocomposites were prepared by melt mixing in a Haake Polydrive two-blade counter-rotating system. The mixing temperature was kept at 200°C to ensure the right viscosity for the mixing while minimizing degradation. The rotation speed was set at 75 rpm. After all ingredients were introduced into the mixing chamber, melt mixing was continued for a period of 5 min. The total weight of the material per batch was 35 g, which gives a suitable volume for the Haake Polydrive mixer. In all nanocomposites, both 0.1 wt % Irganox 1010 and 0.1 wt % calcium stearate were added as stabilizers for the polypropylene matrix.

Unoriented sheets of approximately 0.8 mm thickness were compression molded between brass plates and mylar foil. The temperature for both upper and lower plates was kept at 200°C during molding. The polymer was melted under atmospheric pressure, and, subsequently, the pressure was increased to a maximum of 300 bar. Finally, the sheets were cooled in the compression molder with a flow of cooling water.

Square specimens of 85 mm × 85 mm were cut from the compression-molded sheets and were sequentially biaxially stretched in a Karo IV laboratory stretching machine (Brückner) at a temperature of 160°C and an engineering strain rate of 100% sec^{-1} based on the original specimen dimensions. The preheat time before drawing was fixed at 1.5 min. Films were drawn to target stretching ratio of 5 × 5. After stretching, films of approximately 30-μm thickness were obtained.

Oxygen permeability measurements

The oxygen permeability of the film was measured according to the procedure and instrument

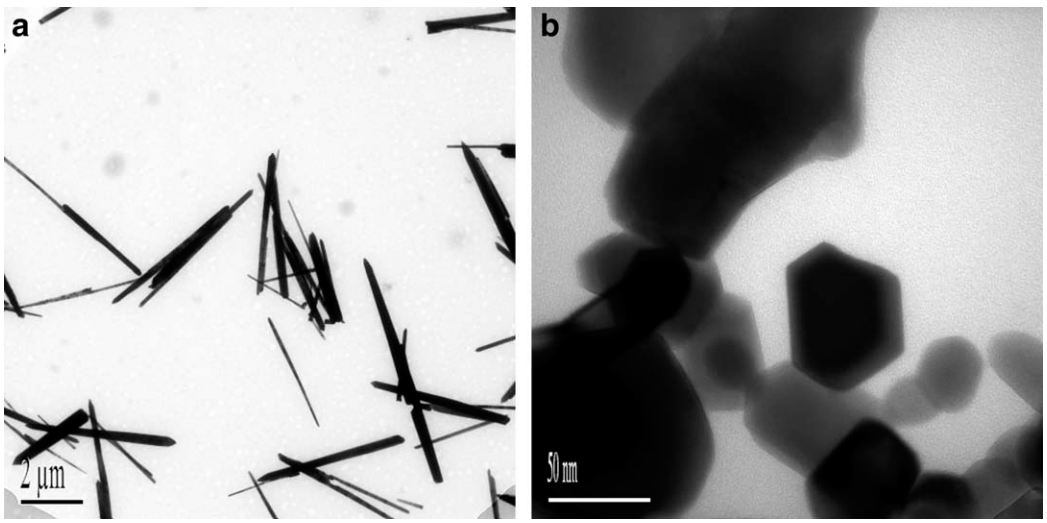

Figure 1 Transmission electron microscopy analysis of elongated (a) and spherical (b) ZnO nanoparticles.

described in ASTM D 3985[30] using an OX-TRAN model 702 of the Mocon Corp. (Minneapolis, MN). Each film was placed on a stainless steel mask with an open testing area of 5 cm^2. One side of the film was exposed to flowing nitrogen gas, and the other side was exposed to 100% flowing oxygen gas under the desired conditions. The system was programmed to have a 4 hr waiting period to allow the films to achieve equilibrium with the controlled temperature of 23°C and 0% relative humidity. Oxygen permeability was calculated by dividing the oxygen transmission rate by oxygen partial pressure and multiplying by the film thickness. Gas permeation experiments were performed more than three times, and the reported values are the mean of the measurements with standard deviations.

Mechanical properties

Measurements of the mechanical properties, Young's modulus and tensile strength at break, were performed on a MTS/10 tensile tester using a crosshead speed of 50 mm/min with a 100-N load cell and a gauge length of 50 mm. Tensile tests were carried out at 23°C and 50% relative humidity. Tensile test specimens were prepared as strips with 15 mm in width according to ISO 1184.[31] Five specimens were tested for each ZnO-BOPP nanocomposite, and the mean values and standard deviations were reported.

Scanning electron microscopy

A FEI Quanta 200 FEG-SEM scanning electron microscope equipped with secondary electron and back scattered electron detectors was used for morphological observation of ZnO-BOPP films and to evaluate the dispersion quality of the ZnO nanoparticles inside the polymeric material. For scanning electron microscopy (SEM) measurements, sections were cut parallel and transverse to the machine stretching direction.

Transmission electron microscopy

The morphology of the nanostructured ZnO material was investigated with a Philips CM12 transmission electron microscopy using an accelerating voltage of 120 kV. For this analysis, the powder is dispersed in methanol, dropped onto a Formvar/carbon 200 Mesh Cu-coated grid and dried at room temperature.

Differential scanning calorimetry

Differential scanning calorimetry (DSC) analyses were carried out to obtain the crystallization and melting curves (DSC measurements performed 1 week after sample preparation) and were carried out with a Perkin–Elmer DSC thermal analyzer under flowing nitrogen atmosphere. The samples were heated to 225°C at 10°C/min and kept at this temperature for 5 min before cooling down to assure that the materials melted uniformly and to eliminate the thermal history. The sample was cooled down to room temperature at a cooling rate of 10°C/min. From the crystallization curves that were recorded, crystallization temperature (T_c) and crystallinity degree can be obtained. Melting temperature (T_m) was detected under the same conditions at a heating rate of 10°C/min.

To estimate the % of crystallinity (χ), the following equation was used:

$$\chi = \frac{\Delta H}{\Delta H_{100}} 100\%$$

where ΔH is the heat of crystallization of the sample analyzed (J/g) and ΔH_{100} is a reference value that

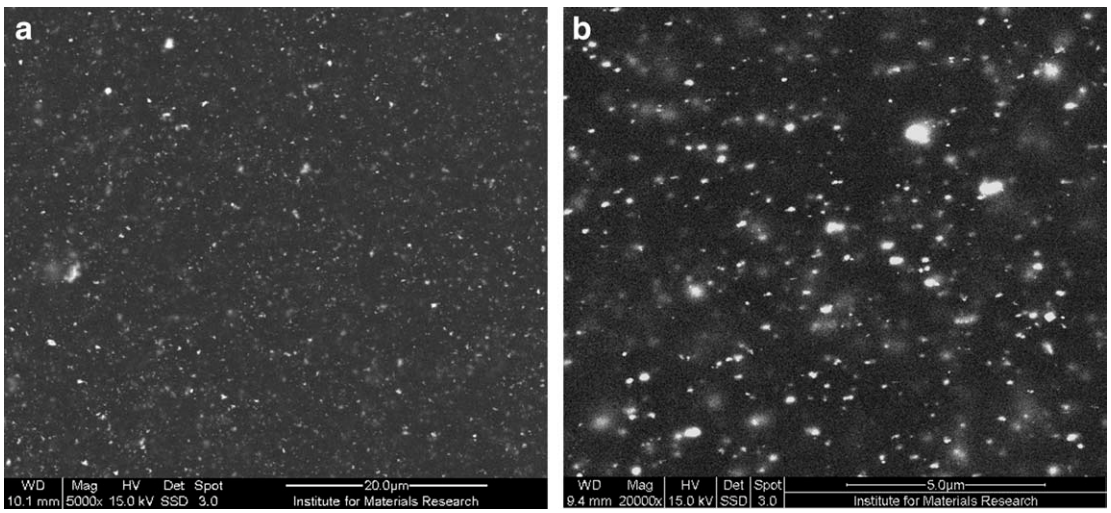

Figure 2 SEM analysis: (a) Surface of ZnO-BOPP nanocomposite with spherical ZnO (5 wt%). (b) Cross-section of ZnO-BOPP nanocomposite, parallel to the orientation in machine direction (i.e., perpendicular to machine direction).

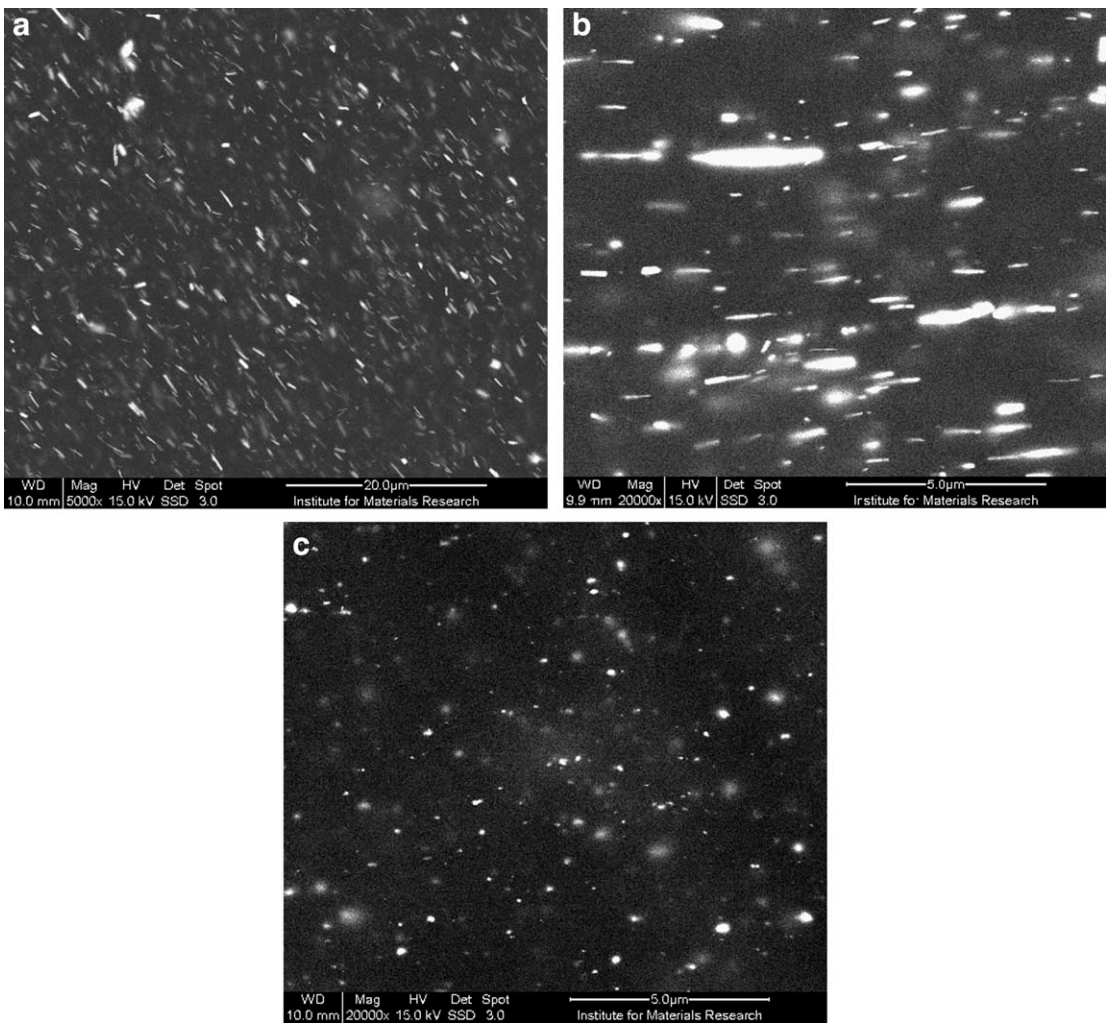

Figure 3 SEM analysis: (a) Surface of ZnO-BOPP nanocomposite with elongated ZnO (5 wt%). (b) Cross-section of ZnO-BOPP nanocomposite, parallel to the orientation in machine direction. (c) Cross-section of ZnO-BOPP nanocomposite, perpendicular to the orientation in machine direction.

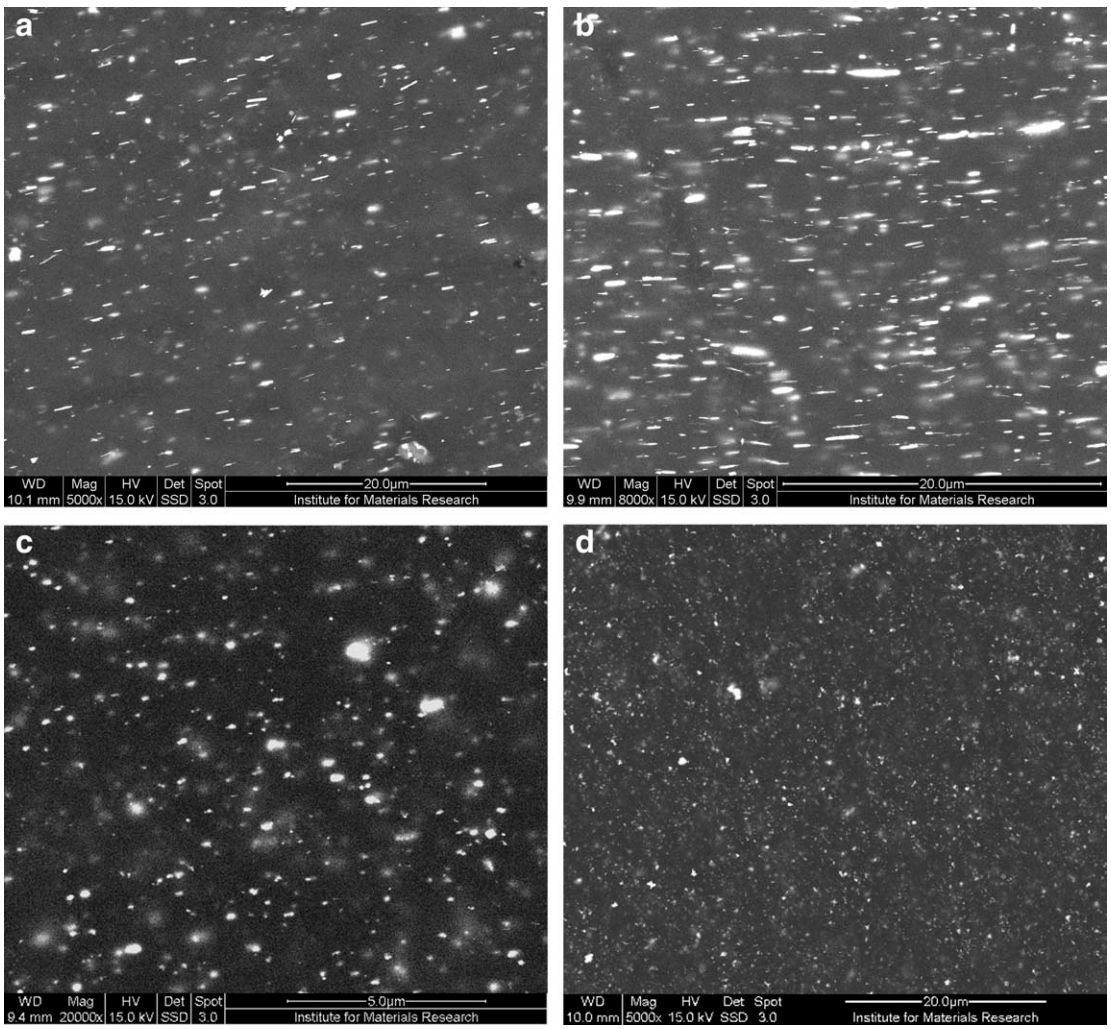

Figure 4 SEM surface analysis of ZnO-BOPP nanocomposites with elongated [(a), 2 wt %; (b), 7.5 wt %] and spherical [(c), 2 wt %; (d), 7.5 wt %] ZnO nanoparticles.

represents the heat of crystallization for a 100% crystalline polymer. For PP, ΔH_{100} is 209 J/g.[21]

RESULTS AND DISCUSSION

Crystallization and morphological characteristics

The oriented films remained clear with no stress whitening, indicating the absence of microvoiding. To confirm this observation, SEM micrographs of surfaces and cross-sections (parallel and transverse to the machine direction [MD]) of ZnO-BOPP nanocomposites containing 5 wt % ZnO spherical or elongated nanoparticles are presented in Figures 2 and 3, respectively. Moreover, transmission electron microscopy images of the spherical ZnO nanoparticles and the ZnO nanorods are shown in Figure 1(a,b), respectively, to reveal the state of the agglomeration of the nanoparticles.

From SEM images it can be concluded that the 1D ZnO nanorods are homogeneously dispersed in the polymer matrix as individual particles. Biaxial orientation of the sheets results in an orientation of the ZnO nanorods in the MD, and no pores or cracks can be observed in the polymer matrix. SEM images of nanocomposites containing spherical ZnO nanoparticles show also good dispersion of the nanoparticles, with only a few areas of agglomerates of a few micrometer; however, these agglomerates did not cause voids or cracks after orientation. Spherical ZnO nanoparticles have a higher tendency to create agglomerates because of their higher surface area compared with 1D ZnO nanorods with the same diameter. Different ZnO-BOPP nanocomposite films with varying ZnO concentrations up to 7.5 wt % have been analyzed with SEM; all of them show similar results (Fig. 4).

To investigate the effect of the ZnO nanoparticles on the melting and the crystallization behavior of biaxially oriented iPP, DSC experiments were performed. Melting point temperatures and crystallinity are presented in Table I. Although the melting

TABLE I
DSC Characteristics of ZnO-BOPP Nanocomposites

Nanocomposite	χ_c (%)	T_m (°C)
Neat iPP	50 ± 0.9	161 ± 0.2
Neat BOPP	56 ± 0.2	168 ± 0.8
BOPP + 2 wt % spherical ZnO	53 ± 0.5	165 ± 0.3
BOPP + 5 wt % spherical ZnO	47 ± 0.5	163 ± 0.1
BOPP + 7,5 wt % spherical ZnO	46 ± 0.4	163 ± 0.3
BOPP + 2 wt % ZnO nanorods	51 ± 0.7	166 ± 0.3
BOPP + 5 wt % ZnO nanorods	50 ± 0.9	164 ± 0.2
BOPP + 7,5 wt % ZnO nanorods	49 ± 0.6	164 ± 0.6

temperature of the neat iPP film was observed at about 161°C, it changes to 168°C in the neat BOPP film after drawing at 160°C. According to Lüpke et al.[15] it is assumed that the increased melting temperature for neat BOPP results from an increased size of the crystallites after deformation at elevated temperatures.

The melting temperatures show a decrease after addition of ZnO nanoparticles because of a decrease in lamellar thickness of the polymer crystals in comparison with neat BOPP.[16,32] From Figure 5 it can concluded that the values of crystallinity increased for the ZnO-iPP nanocomposites after biaxial drawing; both spherical and elongated ZnO nanoparticles show the same trend.

However, after addition of ZnO nanoparticles, crystallinity shows a decreasing trend with increasing wt % of ZnO. According to Li et al.,[33] the changes in the crystallization behavior can be explained by the fact that, because of the good interaction between the ZnO nanoparticles and polypropylene, the mobility of the iPP chains is restricted.

Effect of ZnO nanoparticles and orientation on mechanical and oxygen barrier properties of polypropylene

Tensile tests of ZnO-iPP and ZnO-BOPP films were conducted to determine how mechanical properties were influenced through the incorporation of ZnO nanoparticles and the deformation process. Therefore, Young's modulus and tensile strength at break were investigated as a function of the ZnO incorporation in a iPP and BOPP matrix; results are reported in Figures 6 and 7, respectively.

In general, it can be concluded that the Young's modulus (Fig. 6) of the nanocomposites gradually increases by increasing the ZnO content. The increase in Young's modulus of the ZnO-filled nanocomposites indicates an increase in the rigidity of the polypropylene related to the restriction of the mobility of the polypropylene matrix because of the presence of the fillers.[34] The prepared ZnO-BOPP nanocomposites present significant improvement of Young's modulus with respect to pure BOPP and ZnO-iPP nanocomposites. However, difference can be observed in machine direction (MD) and in transverse direction (TD), depending on the shape of the ZnO nanoparticles. The BOPP nanocomposites with spherical ZnO nanoparticles reach maximum values for Young's modulus in TD, whereas a decrease in Young's modulus in TD is observed for ZnO nanorods [Fig. 6(a)] because of the high orientation of the ZnO nanorods during biaxial orientation and, thus, a maximum strength only in the MD.

Figure 7 illustrates the tensile strength at break values for the nanocomposites with different wt % ZnO. As seen in Figure 7, maximum tensile strength values in MD were obtained at ZnO concentrations of 5 wt %, for both spherical [Fig. 7(b)] and elongated [Fig. 7(a)] ZnO nanoparticles. The tensile strength at break values show a decreasing trend in MD as the wt % ZnO further increases. This behavior is due to the interactions between the nanoparticles as more agglomerates are formed, which act as stress concentrators[9] and to the reduction in effective polymer matrix cross-section.[35] Similar to the results obtained for the Young's modulus of ZnO-BOPP nanocomposites in TD, Figure 7 shows that the tensile strength in case of spherical ZnO in TD is higher than MD; the opposite is true in case of ZnO nanorods.

Oxygen permeability results for pure iPP, ZnO-iPP nanocomposites, and ZnO-BOPP nanocomposites are

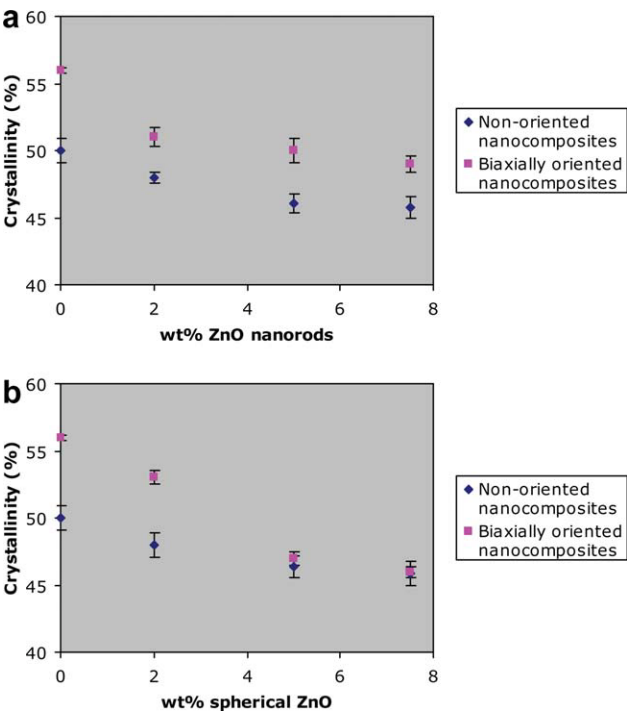

Figure 5 Influence of elongated (a) and spherical (b) ZnO nanoparticles on the crystallinity of the nanocomposites. [Color figure can be viewed in the online issue, which is available at wileyonlinelibrary.com.]

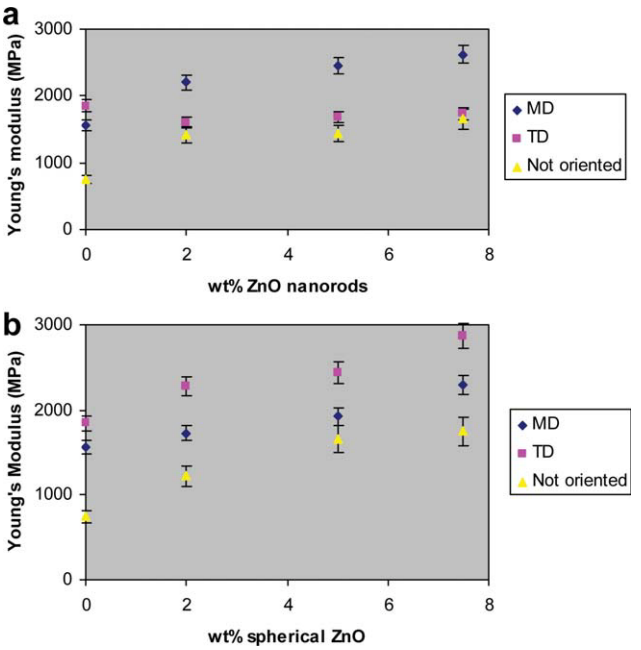

Figure 6 Young's modulus (MPa) versus wt % ZnO. (a) Orientation machine direction. (b) Orientation transverse direction. [Color figure can be viewed in the online issue, which is available at wileyonlinelibrary.com.]

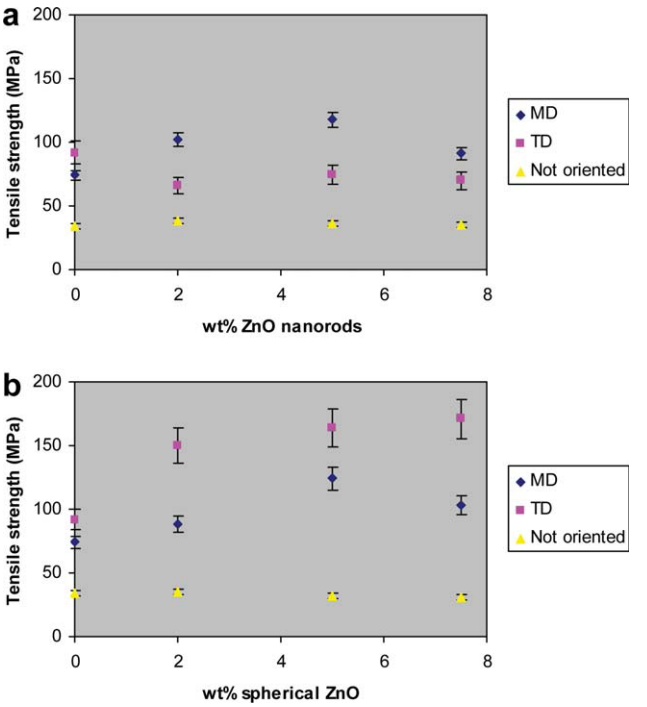

Figure 7 Tensile strength (MPa) versus wt % ZnO. (a) Orientation machine direction. (b) Orientation transverse direction. [Color figure can be viewed in the online issue, which is available at wileyonlinelibrary.com.]

presented in Figure 8. Values, corresponding to the pure iPP, fit well with those given in the literature for poorly oriented iPP.[36] Adding inorganic nanoparticles, such as ZnO, to an oriented polymer film, could improve barrier properties because of the combination of two phenomena:

1. The decrease in area available for diffusion, a result of two effects namely impermeable nanoparticles replacing permeable polymer and the biaxial orientation of the polymer chains.
2. The increase in distance a permeant must travel to cross the film because it follows a tortuous path around the impermeable nanoparticles.

In summary, the oxygen permeability ranges from 51 to 55 mL/(m^2 day) for ZnO-iPP nanocomposites and from 30 to 35 mL/(m^2 day) for ZnO-BOPP, with virtually no correlation with the ZnO concentration. Moreover, elongated and spherical ZnO nanoparticles in iPP and BOPP nanocomposites show the same trend in oxygen permeability; no influence of the nanoparticle shape could be observed. The higher the aspect ratio of the filler, the more tortuous the path; hence, the greater the decrease in permeability. The elongated and spherical ZnO nanoparticles used in this study are not considered the most effective barrier as in the case of sheet-like nanoparticles.[6] By comparing the oxygen permeability of ZnO-iPP with ZnO-BOPP nanocomposites it becomes obvious that

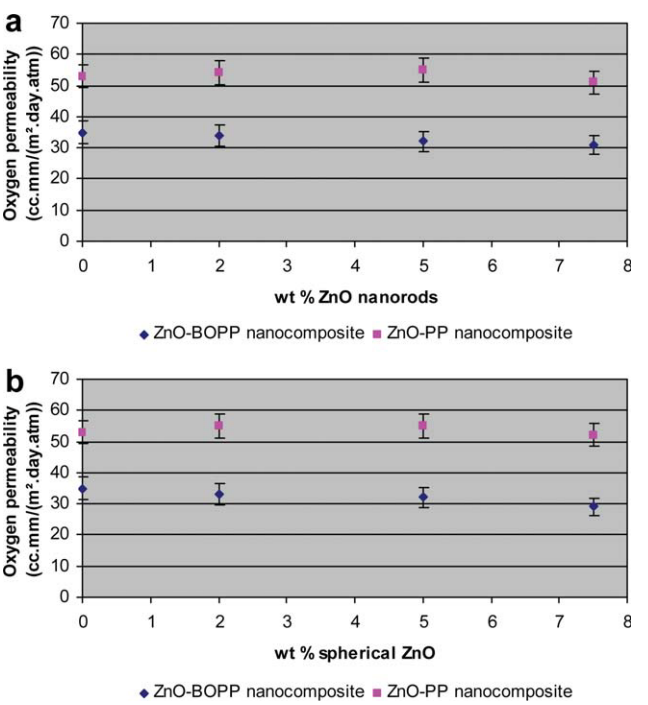

Figure 8 Permeability of O_2 gas of ZnO-PP and ZnO-BOPP nanocomposites as a function of the filler content. (a) ZnO nanorods. (b) Spherical ZnO. [Color figure can be viewed in the online issue, which is available at wileyonlinelibrary.com.]

the biaxially oriented samples show a decrease in oxygen permeability. It is well known that biaxial drawing of the iPP films decreases the gas permeability; the reduction in oxygen permeability is caused by a reduction in gas diffusion.[37]

CONCLUSIONS

Polypropylene nanocomposites filled with 0, 2, 5, and 7.5 wt % ZnO nanoparticles (spherical and elongated) were compounded by a melt mixing process. After melt compounding, ZnO-PP nanocomposite films were compression molded and biaxially stretched.

The effects of the ZnO addition on the morphological, thermal, mechanical, and barrier properties of ZnO-BOPP nanocomposites have been studied. The following conclusions can be drawn:

1. ZnO-BOPP nanocomposites were successfully prepared with a uniform dispersion of the ZnO nanoparticles; no microvoids were observed.
2. The obtained nanocomposites showed enhanced mechanical properties: the oriented ZnO nanocomposite films have markedly improved mechanical properties in both machine and transverse directions for spherical ZnO nanoparticles and specifically in MD for the ZnO nanorods, compared with unfilled BOPP.

In combination with the oxygen barrier properties and with the retention of thermal stability, this is a good development in the field of toughened BOPP materials. This will provide new ideas for further nanocomposite development, and ongoing research in combination with industrial processing methods for food packaging is essential.

The authors are grateful to Borealis Polymers NV (Beringen, Belgium) for providing them with iPP samples and for the assistance in use of their facilities.

References

1. Demjen, Z.; Pukanszky, B.; Nagy, J. Compos Part A 1998, 29, 323.
2. Weidenfeller, B.; Höfer, M.; Schilling, F. R. Compos Part A 2004, 35, 423.
3. Galgali, G.; Agarwal, S.; Lele, A. Polymer 2004, 45, 6059.
4. Ingram, J.; Zhou, Y.; Jeelani, S.; Lacy, T. Mater Sci Eng A 2008, 489, 99.
5. Perrin-Sarazin, F.; Dorval-Douville, G.; Cole, K. C. Polym Mater Sci Eng 2005, 92, 75.
6. Alexandre, M.; Dubois, P. Mater Sci Eng R 2000, 28, 1.
7. Motha, K.; Hippi, U.; Hakkala, K.; Peltonen, M.; Ojanpera, V. J Appl Polym Sci 2004, 94, 1094.
8. Vaia, R. A.; Giannelis, E. P. MRS Bull 2001, 26, 394.
9. Vassiliou, A. Compos Sci Technol 2008, 68, 933.
10. Ellis, T. S.; D'Angelo, J. S. J Appl Polym Sci 2003, 90, 1639.
11. Chu, F.; Kimura, Y. Polymer 1996, 37, 573.
12. Lee, J.; Son, S.; Hong, S. J Food Eng 2008, 86, 484.
13. Dias, P.; Lin, Y.; Hiltner, A.; Baer, E.; Chen, H.; Chum, S. J Appl Polym Sci 2008, 107, 1730.
14. Somlai, L.; Liu, R.; Lardell, L.; Hiltner, A.; Baer, E. J Polym Sci Part B: Polym Phys 2005, 43, 1230.
15. Lüpke, T.; Dunger, S.; Sänze, J.; Rodush, H. Polymer 2004, 45, 6861.
16. Krump, H.; Luyt, A.; Hudec, I. Mater Lett 2006, 60, 2877.
17. Paiva, L. B.; Morales, A.; Guimaraes, T. Mater Sci Eng A 2007, 447, 261.
18. García-Lópeza, D.; Picazo, O.; Merino, J.; Pastor, J. Eur Polym J 2003, 39, 945.
19. Manias, E.; et al. Polym Mater Sci Eng 2000, 82, 282.
20. Tang, J.; Wang, Y.; Liu, H. Polymer 2004, 45, 2081.
21. Garcia, M. Rev Adv Mater Sci 2004, 6, 169.
22. Chan, C.; Wu, J.; Li, J.; Cheung, Y. Polymer 2002, 43, 2981.
23. Bertini, F.; Canetti, M.; Audisio, G. Polym Degrad Stab 2006, 91, 600.
24. Kotek, J.; Kelnar, I.; Studenovsky, M.; Baldrian, J. Polymer 2005, 46, 4876.
25. Giannelis, E. P.; Krishnamoorti, R.; Manias, E. Adv Polym Sci 1999, 138, 107.
26. Huang, C.; Chen, S.; Wei, W. J Appl Polym Sci 2006, 102, 6009.
27. Demjén, Z.; Pukanszky, B. Polym Compos 1997, 18, 741.
28. Zhao, H.; Li, R. Polymer 2006, 47, 3207.
29. Lepot, N.; Van Bael, M.; Van den Rul, H.; D'Haen, J.; Peeters, R.; Franco, D.; Mullens, J. Mater Lett 2007, 61, 2624.
30. ASTM. ASTM D 3985-05. Standard Test Method for Oxygen Gas Transmission Rate through Plastic Film and Sheeting Using a Coulometric Sensor. ASTM: Washingto, DC.
31. ISO. ISO 1184. Plastics—Determination of Tensile Properties of Films; ISO: Geneva, Switzerland, 1983.
32. Behrendt, N.; Mohmeyer, N.; Hillerbrand, J.; Klaiber, M. J Appl Polym Sci 2006, 99, 650.
33. Li, P.; Song, G.; Yin, L.; Wang, L.; Ma, G. J Appl Polym Sci 2008, 108, 2116.
34. Metin, D.; Timinlioglu, F.; Balköse, D.; Ülkü, S. Compos Part A 2004, 35, 23.
35. Nielsen, L. J Appl Polym Sci 1996, 10, 97.
36. Taraiya, A. K. G.; Orchard, A. J.; Ward, I. M. J Appl Polym Sci 1990, 41, 1659.
37. Vladimirov, V.; Betchev, C.; Vassiliou, A.; Papageorgiou, G.; Bikiaris, D. Compos Sci Technol 2006, 66, 2935.